Article

Close Observation of the Evolution Process during Initial Stage of Triggered Lightning Based on Continuous Interferometer

Zefang Chen [1,2], Yang Zhang [1,*], Yanfeng Fan [1], Jingxuan Wang [1,3], Weitao Lyu [1], Dong Zheng [1] and Wenjing Pang [2]

1   State Key Laboratory of Severe Weather, Chinese Academy of Meteorological Sciences, Beijing 100081, China; chenzf@cma.gov.cn (Z.C.); fanyf@cma.gov.cn (Y.F.); 3190301007@stu.cuit.edu.cn (J.W.); wtlyu@cma.gov.cn (W.L.); zhengdong@cma.gov.cn (D.Z.)
2   Meteorological Observation Centre, China Meteorological Administration, Beijing 100081, China; pwjaoc@cma.gov.cn
3   College of Electronic Engineering, Chengdu University of Information Technology, Chengdu 610225, China
*   Correspondence: zhangyang@cma.gov.cn

Abstract: The discharge signal in the initial stage of lightning is weak. The revelation of the discharge mechanism at this stage depends especially on close observation. In this study, a continuous interferometer (CINTF) was used to observe the initial stage of the upward positive leader (UPL) of the triggered lightning in Conghua District, Guangzhou City, Guangdong Province. The positioning error of CINTF for a close-range radiation source was analyzed, and the positioning error calibration method of CINTF for a specific close-range radiation source was studied, which improved the observation accuracy of elevation angle at the initial stage of the UPL of the triggered lightning. With the rise of the rocket, the positioning error in altitude during the initial stage of the UPL increased obviously. Under the layout condition of the Guangzhou field experiment site for lightning research, when the positioning results of the elevation angle of the initial stage of the UPL were $40°$, $50°$, and $60°$, respectively, the calibrated altitude positioning error could be reduced by about 11 m, 14 m, and 20 m, respectively. On the basis of the calibrated observation results, the evolution characteristics of the initial stage of the UPL were studied, and its discharge mechanism was revealed. The precursor current pulse (PCP) was generated by a weak upward positive breakdown and a subsequent strong downward negative breakdown near the rising rocket tip, which was in the form of a single pulse. The precursor current pulse cluster (PCP cluster) and initial precursor current pulse cluster (IPCP) were both signs of self-sustaining development of the UPL. After the PCP cluster, self-sustaining development stopped immediately. The self-sustaining development after IPCP could be short-term or continuous.

Keywords: triggered lightning; upward positive leader; initial stage; continuous interferometer

1. Introduction

The upward positive leader (UPL) process determines the position of return strokes of negative cloud-to-ground (CG) lightning. However, due to the uncertain location and short transmission distance of UPL, it is very difficult to observe. Up to now, the understanding of the occurrence, development, and transmission process of UPL is still very limited. The research on UPL is an important issue in the research of lightning physics and lightning protection. Triggered lightning can provide a discharge process similar to natural lightning, and its occurrence time can be known, its location can be determined, and its discharge parameters are convenient for close observation. Therefore, it has become an important means to study the discharge process of UPL.

The UPL includes two stages: the initial stage and the self-sustaining development stage. The discharge signal during the initial stage is very weak. Thus, it is difficult to detect. At present, the limited research is mainly based on directly measured current of

triggered lightning. Horii [1] first introduced PCP and found that PCP appeared in the form of a single element or group, and the amplitude was less than 100 A. Willett et al. [2] found that the individual current impulses that make up a precursor tend to be separated by roughly 30 ms, whereas the interval between the precursors themselves tends to be on the order of 10 ms. Zhang et al. [3] statistical analysis showed that the geometric mean values of current peak, 10–90% rise time, duration, half peak width, transferred charge, and pulse interval for the pulses generated before the appearance of the continuously upward leader are 28 A, 0.33 μs, 2.3 μs, 0.73 μs, 27 μC, and 25 μs, respectively. Chen et al. [4] found that the initial stage of triggered lightning can be divided into two types: single initial process form and multiple initial process form. In each initial process, the current waveform changes with the development of the UPL, mainly including PCP, PCP cluster, and IPCP. When the pulse duration and transferred charge of a PCP increase to a certain extent, PCP clusters and IPCPs begin to appear. After the IPCP, the UPL begins self-sustaining development, and the current waveform is no longer in the form of pulse, but in the form of continuous current, i.e., initial continuous current (ICC). According to the analysis of six negative triggered flashes, Li et al. [5] found that both precursor discharges and the initial upward leader begin with a small pulse that leads the subsequent major pulses by about 25 μs.

With the development of lightning very-high-frequency (VHF) positioning technology, researchers began using VHF positioning systems to study the positive leader. Shao et al. [6] found that the observations for most of the +CGs showed complete lack of radiation a few ms before the beginning of the return strokes, suggesting that the ongoing downward positive leaders were quiet at VHF, at least during the final few ms. Ushio et al. [7] used a broadband interferometer and observed that the radiation signal of the positive leader could not be detected in either natural lightning or triggered lightning. In the artificially triggered lightning experiment in the summer of 1999, Dong et al. [8] used an improved broadband interferometer to detect the VHF radiation signal of the UPL for the first time, and obtained the two-dimensional positioning results. At the same time, it was found that there are few channel bifurcations during the development of UPL, and the initial development speed is on the order of 10^5 m/s. Yoshida et al. [9] found that the locatable VHF sources of two UPLs began at 1.1 km and 1.5 km, a few milliseconds after the UPL inception, and ascended to 2.4 km and 3.7 km, respectively, with average 3D speeds on the order of 10^6 m/s. VHF sources associated with positive leader propagation were located when the average current was higher than 3 kA and had significant pulse activity. Edens et al. [10] found that the UPL initiated at 3.4 km altitude, but was mapped only above 4.0 km altitude after the onset of retrograde negative breakdown, indicating a change in leader propagation and VHF emissions. Their observation results also suggested that both positive and negative breakdown produce VHF emissions that can be located by time-of-arrival systems, and that not all VHF emissions occurring along positive leader channels are associated with retrograde negative breakdown. Hill et al. [11] found that the initial stage of Florida triggered lightning typically transitions from vertical to horizontal propagation at altitudes of 3–6 km, near the typical freezing level of 4 km and several kilometers below the expected center of the negative cloud-charge region at 7–8 km. LMA source locations were obtained from VHF sources of positive impulsive currents as small as 10 A. Hill et al. [12] found that the initial stage of each flash propagated generally vertically to the altitude of the 0 °C melting level, about 5 km, and then subsequently propagated for many kilometers horizontally along the melting level contour. Sun et al. [13] found that the UPL was mapped immediately from the tip of the metal wire during the initial stage, developing at a speed of about 10^4 m/s without branches. The UPL and all 14 negative leaders captured by the 2D imaging system propagated along the same channel with few branches inside the cloud. Zhang et al. [14] found that the PCPs were produced by breakdown at the ascending tip of the rocket, and that individual PCPs were produced by weak upward positive breakdown over meter-scale distances, followed by more energetic, fast downward negative breakdown over several tens of meters by interferometer observation.

Some studies provided the current characteristics, development speed, and development form of the UPL through observation, and analyzed the self-sustaining development process of the UPL, but the research on the evolution of the initial stage before self-sustaining development is still very limited. In addition, although a continuous interferometer (CINTF) can finely observe the initial stage of close-range triggered lightning, the current location method has some errors in locating close-range breakdown discharge events, which needs to be further improved. Therefore, this paper proposes a positioning error calibration method of CINTF for a specific close-range radiation source. On the basis of the work of Chen et al. [4], the physical process during the initial stage of the UPL of artificially triggered lightning is studied through CINTF observation.

2. Experiment and Data

Since 2006, the lightning research group of Chinese Academy of Meteorological Sciences has carried out triggered lightning experiments in Conghua District, Guangzhou City. More information about this experiment can be found in [15]. The schematic diagram of the experiment site is shown in Figure 1. Since 2016, a CINTF has been set up at the experiment site, which is about 90 m away from the rocket launch and current measurement area. It continuously locates the whole discharge process of triggering lightning by detecting VHF broadband signals. The CINTF mainly includes indoor acquisition and recording equipment and outdoor antennas. In this paper, the three antennas ⑤–⑦ in Figure 1 are defined as antenna A, antenna B, and antenna C, respectively. They are respectively located at the three vertices of an equilateral triangle with a side length of 20 m, and antenna C is located to the west of antenna A. The signals from each of these VHF antennas were bandpass-filtered to 25–90 MHz and recorded continuously with 16 bit resolution and a sampling rate of 200 MHz. The recorded length was 4 s with a trigger length of 2 s, which could realize the complete observation and recording of the whole process of triggered lightning. More information about the CINTF is provided in [14,16]. The data used in this paper also include directly measured current and fast electric field change. The related information can be found in [4,16–20].
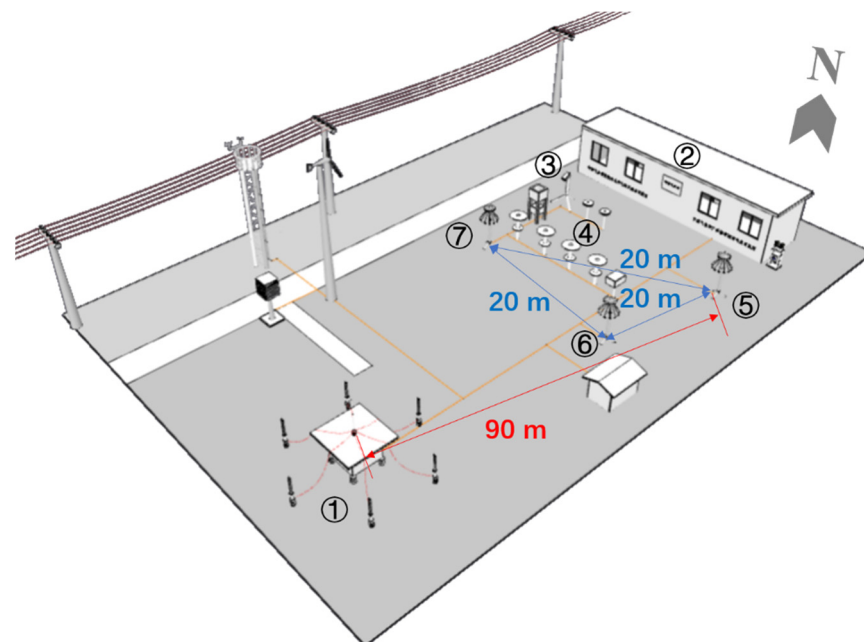

Figure 1. Schematic diagram of Guangzhou field experiment site for lightning research. ① Rocket launch and current measurement area. ② Control room. ③ Atmospheric electric field meter. ④ Electric field and magnetic field observation area. ⑤–⑦ Antennas of CINTF.

3. CINTF Error Calibration for the Initial Stage of the UPL

3.1. Basic Principle of CINTF Positioning

The principle is illustrated in Figure 2. Two broadband antennas A and B at a certain distance constitute the simplest broadband interferometer system. Usually, the distance from the lightning breakdown discharge event to the CINTF antenna is much longer than the baseline length; hence, its VHF radiation can be regarded as a plane wave. Assuming that the incident angle is θ, the time difference Δt between signals arriving at antenna A and antenna B has the following relationship with θ:

$$c \cdot \Delta t = d \cdot \cos \theta, \tag{1}$$

where c is the speed of light. The elevation angle and azimuth angle of the radiation source can be obtained through three antennas' signals (see [14,16,21,22] for more details). The CINTF positioning results shown in this paper all take antenna A as the coordinate origin; the true north direction is the $0°$ azimuth direction, and the true east direction is the $90°$ azimuth direction.
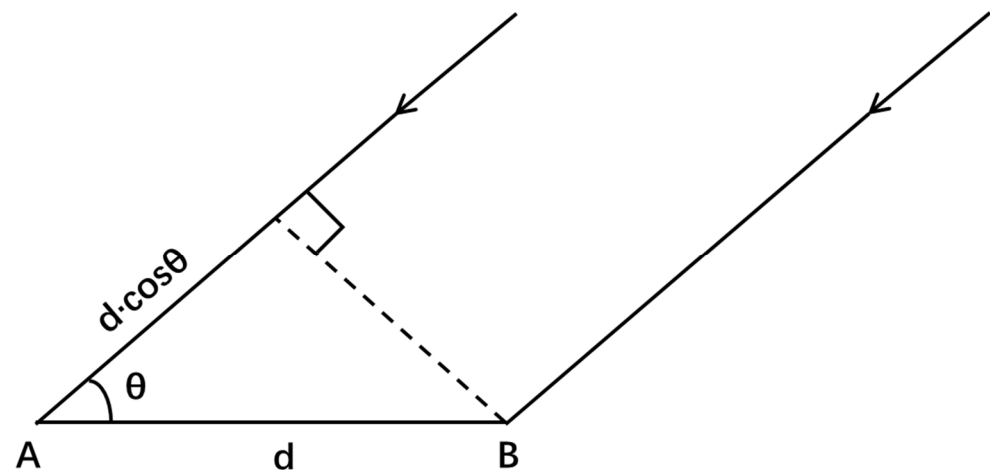

Figure 2. Schematic diagram of CINTF detecting VHF radiation signal.

Only the elevation angle and azimuth angle of the VHF radiation source can be obtained by a single-station CINTF, whereas the actual spatial position cannot be determined. When studying the UPL of artificially triggered lightning, the elevation angle and azimuth angle are usually projected to the position in the space plane, which is convenient to calculate the two-dimensional development speed and length of the radiation source [23,24]. In this paper, the east–west plane perpendicular to the ground at the launching position of the rocket was selected as the abovementioned space plane. The azimuth angle of the rocket launch site was $190°$, and the horizontal distance from the coordinate origin was 90 m. The position of the radiation source on this plane could be determined by the elevation angle and azimuth angle, and then the two-dimensional development speed and length of the radiation source could be calculated.

3.2. CINTF Error Calibration Method for the Initial Stage of the UPL

The method in Section 3.1 is based on the assumption that the distance from lightning radiation source to CINTF antenna is much longer than the antenna baseline length. When the radiation source is close to the CINTF antenna, such as the initiation stage of the UPL of artificially triggered lightning in this paper, the plane wave assumption will bring some errors. For the radiation source during UPL, the real distance difference between the

radiation signal and the two antennas is as follows (as shown in Figure 3), which is not equal to $d \cdot \cos\theta$ in Equation (1):

$$c \cdot \Delta t = |SA| - |SB|, \tag{2}$$

where S is the position of the radiation source. Therefore, calibration is required.
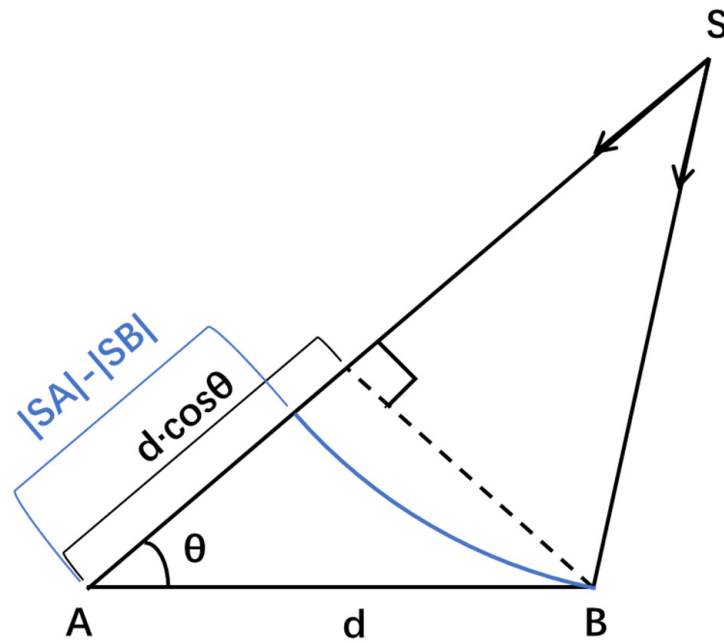

Figure 3. Schematic diagram of CINTF detecting short-range radiation signal.

According to the existing research results, the initial stage of the UPL of artificially triggered lightning generally develops vertically from the rocket launching position under ideal conditions. In practice, due to the influence of atmospheric conditions (such as wind), the ascending path of the rocket may have some deviations from the vertical direction, but the deviation is generally small, less than 10°. We assume that the deviation is 5°; thus, it is estimated that the horizontal component of the path is about one-sixth of the vertical component, which does not affect the conclusion of this paper. Using the elevation angle and azimuth angle of the radiation source obtained by the method in Section 3.1, the actual distance difference between the radiation source position and antennas A and B can be calculated. Then, in the vertical direction of the rocket launching position, the position where the distance difference from antennas A and B is equal to the above actual distance difference can be determine, i.e., the actual radiation source position.

As shown in Figure 4, it is assumed that the position of the radiation source detected by the CINTF at the initial stage of the UPL is S, and its projection on the horizontal plane is S', which is the rocket launching position under the assumption of vertical development. It is known that the distance between S' and the coordinate origin (antenna A) is 90 m, the angle between S'A and due south is 10°, the distance d between antenna A and antenna B is 20 m, and the angle between AB and due west is 60°. At this time, the distance difference between the actual VHF radiation source position and antennas A and B is calculated as follows:

$$c \cdot \Delta t = d \cdot \cos \angle SAB = d \cdot \cos \angle SAS' \cdot \cos \angle BAS', \tag{3}$$

where $\angle SAS'$ is the elevation angle φ detected by CINTF before calibration. $\angle BAS'$ is 20°. It is assumed that the elevation at the actual radiation source position S^* is φ^*. The distance difference between A and B is calculated as follows:

$$|S^*A| - |S^*B| = d \cdot \cos \angle SAS' \cdot \cos \angle BAS'. \tag{4}$$
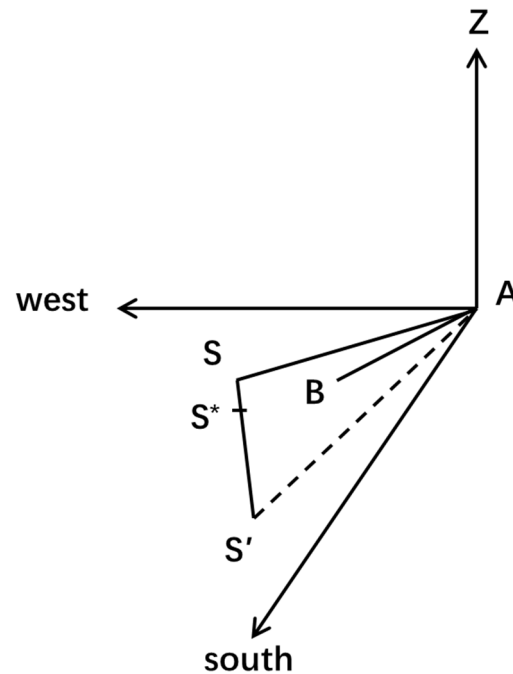

Figure 4. Schematic diagram of radiation source position in the initial stage of the UPL.

The positions of S^*, A, and B can be expressed by space rectangular coordinates. With antenna A as the coordinate origin, due east as the X-axis, due north as the Y-axis, and vertical upward as the Z-axis, the A coordinate is $(0, 0, 0)$, the B coordinate is $(-10, -20\sin 60°, 0)$, and the S^* coordinate is $(-90\sin 10°, -90\cos 10°, 90\tan\varphi^*)$. $|S^*A|$ and $|S^*B|$ are calculated on the basis of space rectangular coordinates. The above equation can be solved to get the calibrated elevation angle φ^*. In this way, the calibration for the CINTF positioning result of the initial stage of UPL is completed.

It should be noted that this calibration method is only aimed at the positioning error of the short-distance breakdown discharge event in the initial stage of the UPL caused by the basic principle of CINTF positioning. Other error sources are not considered in this paper. This method can calibrate the positioning error caused by plane wave hypothesis, and this error is very significant in close observation. This method is suitable for a certain development path. For example, the initial stage of the UPL can be considered as developing directly above the rocket launch position. However, there are limitations in positioning error calibration for uncertain development paths, which still need to be improved. In addition, the positioning results of the initial stage of the UPL shown below were calibrated.

3.3. Analysis of CINTF Positioning Error in Initial Stage of UPL

This section analyzes the influence of the height and distance of the radiation source on the positioning error. Firstly, taking the azimuth direction of the launching position (190°) and the height of the radiation source of 500 m as an example, the vertical error of the positioning results under different projection distances of radiation source was analyzed by changing the distance between CINTF and the launch position. The results are shown in Figure 5. The distance from the projection position of the radiation source on the earth plane to the coordinate origin is defined as the projection distance of the radiation source. When the projection distance of the radiation source was very small, the vertical error

was large, and the vertical error at the distance of 50 m was 135 m, which indicates that is necessary to calibrate the positioning results of the short-range radiation source. With the increase in projection distance, the vertical error showed a downward trend, and the corresponding height error at a distance of 200 m dropped to 29 m. When the projection distance was 1000 m, the vertical positioning error was reduced to 8 m, and the error was obviously smaller at this time, which also shows the reliability of the conventional results of CINTF positioning.
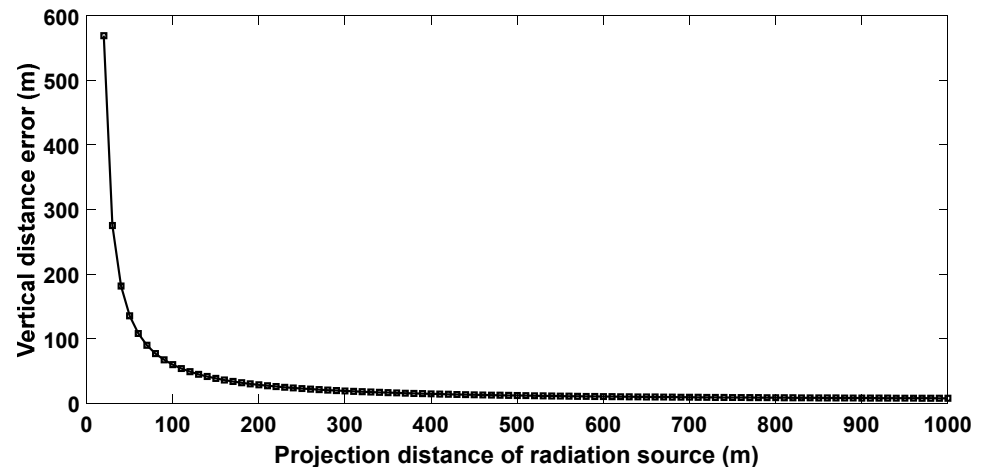

Figure 5. Variation of vertical error with projection distance of radiation source when the height of radiation source is 500 m.

Assuming that the radiation source was located in the vertical direction of the rocket launch site, the vertical error of the positioning results of the radiation source at different heights was analyzed, and the results are shown in Figure 6. The vertical error showed an obvious upward trend with the increase in elevation angle (increase in the height of radiation source). When the elevation angles in the positioning results of the initial stage of UPL were 40°, 50°, and 60°, the vertical distance errors after calibration could be reduced by about 11 m, 14 m, and 20 m, respectively. When the elevation angle was above 70°, the vertical distance error obviously increased.
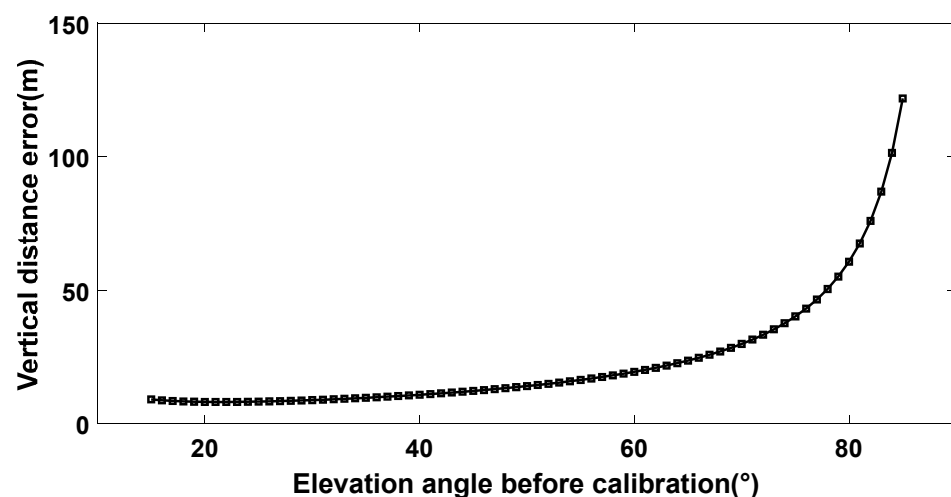

Figure 6. Variation of vertical distance error at launch site with height of radiation source.

4. Evolution Characteristics during Initial Stage of UPL: Results and Discussion

The discharge process including one IPCP–ICC is defined as an initial process. The initial stage of the UPL of triggered lightning can be divided into two types: the single initial process form and the multiple initial process form. The single initial process form has only

one PCP (and PCP cluster)—IPCP–ICC in current waveform. The multiple initial process form has 2–3 PCPs (and PCP clusters)—IPCP–ICC in current waveform. In other words, there will be 1–2 short-term self-sustaining developments in the initial stage of the UPL [4].

4.1. The Single Initial Process Form

This section takes the artificially triggered lightning No. 370 on 4 June 2019 as an example (see [4] for more details about this lightning) and analyzes the overall development process of the initial stage in the single initial process form. In addition, the PCP and IPCP are analyzed in detail.

The positioning results of the VHF radiation source in the initial stage of the triggered lightning are shown in Figure 7. It can be seen that the elevation angle of the radiation source detected by CINTF increased obviously with time, and the azimuth angle changed little with time. This shows that the breakdown discharge event developed approximately vertically upward with the rocket rising, and the approximate development direction is shown by the arrow in Figure 7. At present, related research has reported that the breakdown discharge event in the initial stage of the UPL occurs near the tip of the rising rocket [2,25–28]. Therefore, it can be considered that the development path of the radiation source is basically the same as the ascending path of rocket before the UPL self-sustaining development.
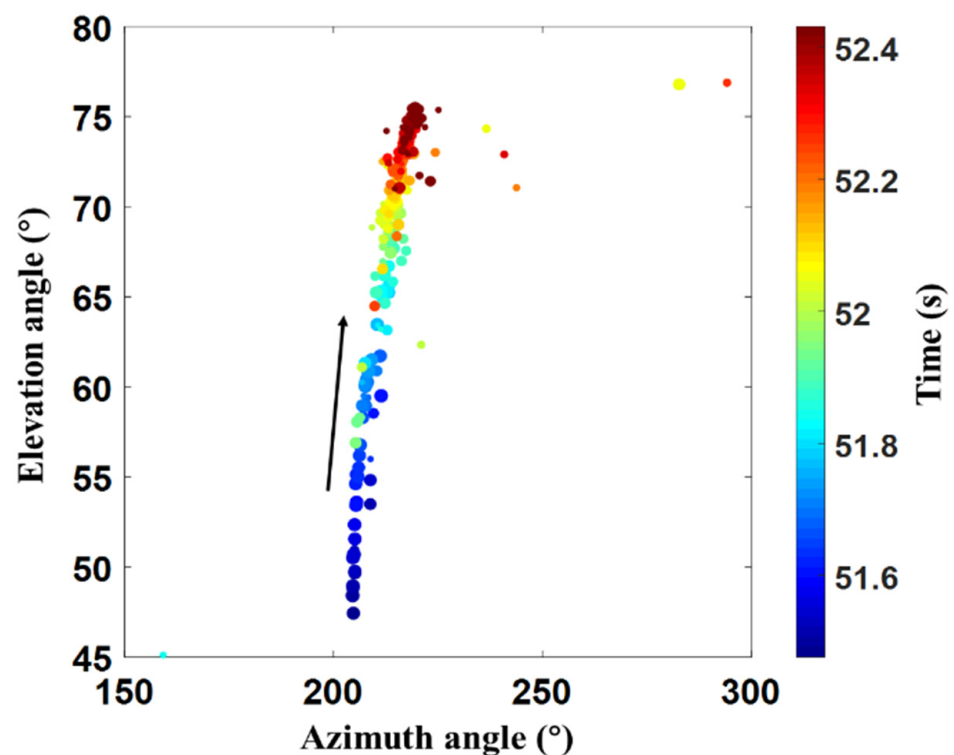

Figure 7. Positioning results of the initial stage of triggered lightning No. 370. The size of the positioning point represents the intensity of VHF radiation, and the color represents time.

The current and elevation positioning results of the VHF radiation source in the initial stage of lightning No. 370 are shown in Figure 8. Considering the observation fact that the initial stage is approximately vertical upward development, the height and development speed of the radiation source can be calculated. The elevation angle of the VHF radiation source detected by CINTF started at about 48°, the height was about 100 m, and the breakdown discharge began near the rocket tip at this time. When developing to IPCP, the elevation angle of the VHF radiation source was about 75°, and the height at this time was about 336 m. The calculated velocity at this stage was about 247 m/s, which is quite

consistent with the rising velocity of the rocket. It also proves that the breakdown discharge occurred near the tip of the rocket.
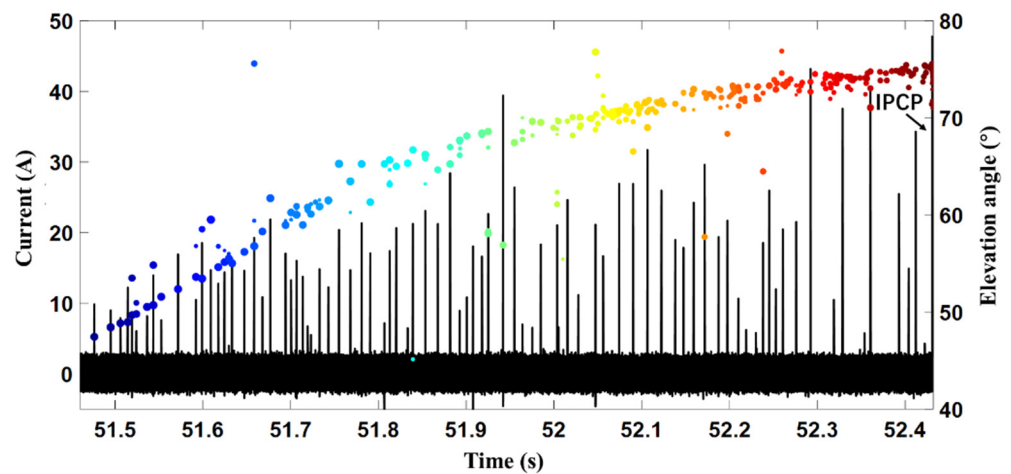

Figure 8. Elevation positioning results and current of the initial stage of triggered lightning No. 370. The size of the positioning point represents the intensity of VHF radiation, and the color represents time.

PCP was produced by weak upward positive breakdown over meter-scale distances, followed by more energetic, fast downward negative breakdown over several tens of meters [14]. Similar results were also obtained in this paper. The current, fast electric field change and radiation source positioning results of a PCP are shown in Figure 9. In this paper, a positive electric field change corresponds to the increase in positive charge or the removal of negative charge above the observation position. Using the analysis method mentioned in [14,29], it is considered that this PCP corresponds to an upward positive breakdown and a downward negative breakdown. Assuming that the development path is vertical, it is calculated that the upward two-dimensional speed was about 2.2×10^7 m/s, the two-dimensional development scale was about 2 m, the downward two-dimensional speed was about 6.8×10^7 m/s, and the two-dimensional development scale was about 28 m.
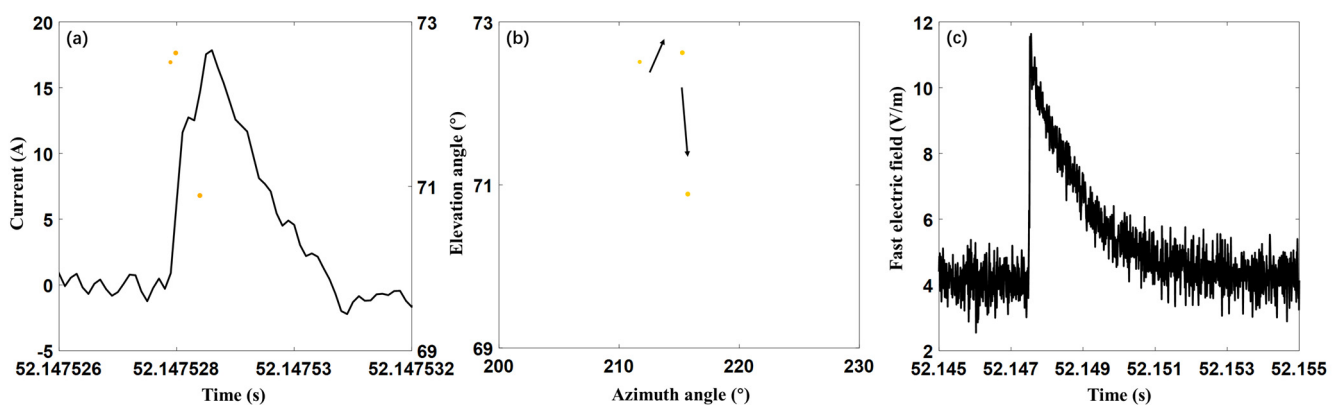

Figure 9. The current waveform (**a**), radiation source positioning results (**b**) and fast electric field change waveform (**c**) of a PCP of lightning No. 370. The size of the positioning point represents the intensity of VHF radiation, and the color represents time.

Through the analysis of several PCPs, it was found that the two-dimensional velocity of five upward positive breakdowns was on the order of 10^6–10^7 m/s, with an average of 8.4×10^6 m/s, and the two-dimensional development scale was in the range of 1–5 m, with an average of 3 m. The two-dimensional velocity of 13 downward negative breakdowns was on the order of 10^6–10^7 m/s, with an average of 4.3×10^7 m/s, and the

two-dimensional development scale was within 40 m, with an average of 15 m. The average speed and development scale of downward negative breakdown were greater than those of upward positive breakdown. It was speculated that the upward process corresponds to the head breakdown process, and the downward recoil process corresponds to the channel establishment process. Zhang et al. [14] analyzed an artificially triggered lightning and found that the average two-dimensional velocity of upward positive breakdown was 5×10^6 m/s, the average two-dimensional development scale was 2.1 m, the average two-dimensional velocity of downward negative breakdown was 3×10^7 m/s, and the average two-dimensional development scale was 20 m. The analysis results are in good agreement with the above results.

At present, relevant research has indicated that the IPCP marks the beginning of self-sustaining development of the UPL [2,3,25,28,30,31]. There was only one IPCP in the initial stage of lightning No. 370, as shown in Figure 10. Before the IPCP, the radiation of breakdown discharge developed upward with the rocket rising, and the development speed was close to that of the rocket rising. During the IPCP process, the two-dimensional development speed calculated on the basis of the elevation angle and azimuth angle of the radiation source detected by CINTF was on the order of 10^5 m/s, which is much faster than the development speed of the initial stage. It shows that the IPCP is obviously different from its previous stage, andthe UPL has started self-sustaining development at this time.
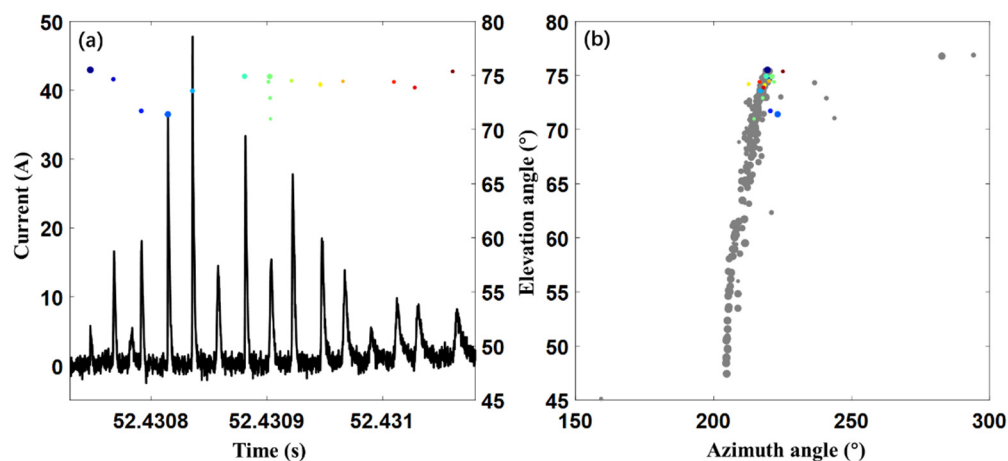

Figure 10. The current waveform and radiation source positioning results of the IPCP of lightning No. 370. (**a**) current waveform and elevation of VHF radiation source versus time; (**b**) elevation of VHF radia-tion sources versus azimuth. The color positioning point is the VHF radiation source of IPCP, and the gray positioning point is the VHF radiation source of the previous initial process. The size of the positioning point represents the intensity of VHF radiation, and the color represents time.

4.2. The Multiple Initial Process Form

Taking the artificially triggered lightning No. 570 on 11 June 2019 as an example (see [4] for more details about this lightning), this section analyzes the overall development process of the initial stage in the multiple initial process form. In addition, PCP cluster and short-term self-sustaining development are analyzed in detail. The PCP and IPCP in lightning No. 570 are similar to those in lightning No. 370; hence, they are not analyzed here.

The positioning results of the VHF radiation source in the initial stage of the triggered lightning are shown in Figure 11. Similar to lightning No. 370 in Section 4.1, the initial stage of lightning No. 570 also developed approximately vertically upward, and the development path was basically the same as the rocket's ascending path.
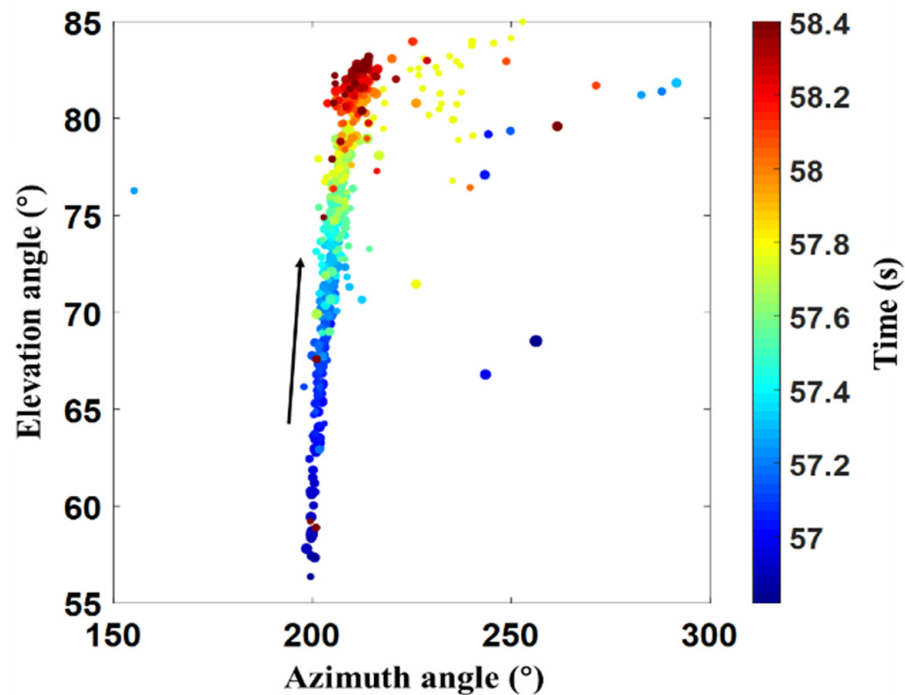
Figure 11. Positioning results of the initial stage of triggered lightning No. 570. The size of the positioning point represents the intensity of VHF radiation, and the color represents time.

The current and elevation positioning results of the VHF radiation source in the initial stage of lightning No. 570 are shown in Figure 12. There were three IPCPs in this lightning, and each IPCP process was followed by an ICC process with different durations. The elevation angle of the radiation source first detected by the CINTF was about 56.5°, and the corresponding height was about 136 m. When developing to the third IPCP, the elevation angle of the radiation source was about 82.5° with a height of about 684 m. The development speed during this stage was about 347 m/s. Although this speed was slightly higher than that of lightning No. 370, there was no difference in the order of magnitude. It may be because the height of this initial stage was higher, and the CINTF has a large positioning error for a radiation source with higher elevation, thus leading to the estimated height and development speed having a large error.

In the initial stage of this artificially triggered lightning, when the first IPCP occurred, the elevation angle of VHF radiation source detected by CINTF was about 76.5° with a corresponding height of 375 m. The UPL started self-sustaining development. The subsequent ICC lasted for 0.34 ms, and the first self-sustaining development ended. However, in Figure 11, there is no obvious radiation source deviated from the channel of initial stage, and this short-term self-sustaining development is further analyzed below.

After the first initial process, there was a quiet period with no obvious pulse in the current waveform, which lasted about 59.08 ms, and no VHF radiation source was detected during this period. This may be because the short-term self-sustaining development reduced the local electric field near the top of the rocket. As the rocket continued to rise, the electric field near the top gradually increased, and, when it reached a certain threshold, the second initial process began. The path of the VHF radiation source detected by the CINTF was continuous with the previous process, and the breakdown still occurred near the rocket tip. When the second IPCP occurred, the elevation angle of the radiation source detected by CINTF was about 80°, and the height at this time was about 510 m. The ICC after the second IPCP lasted about 2.76 ms. At this time, the radiation source detected by the CINTF obviously deviated from the development channel in the initial stage (yellow positioning point in Figure 11). At this time, the breakdown no longer occurred near the tip

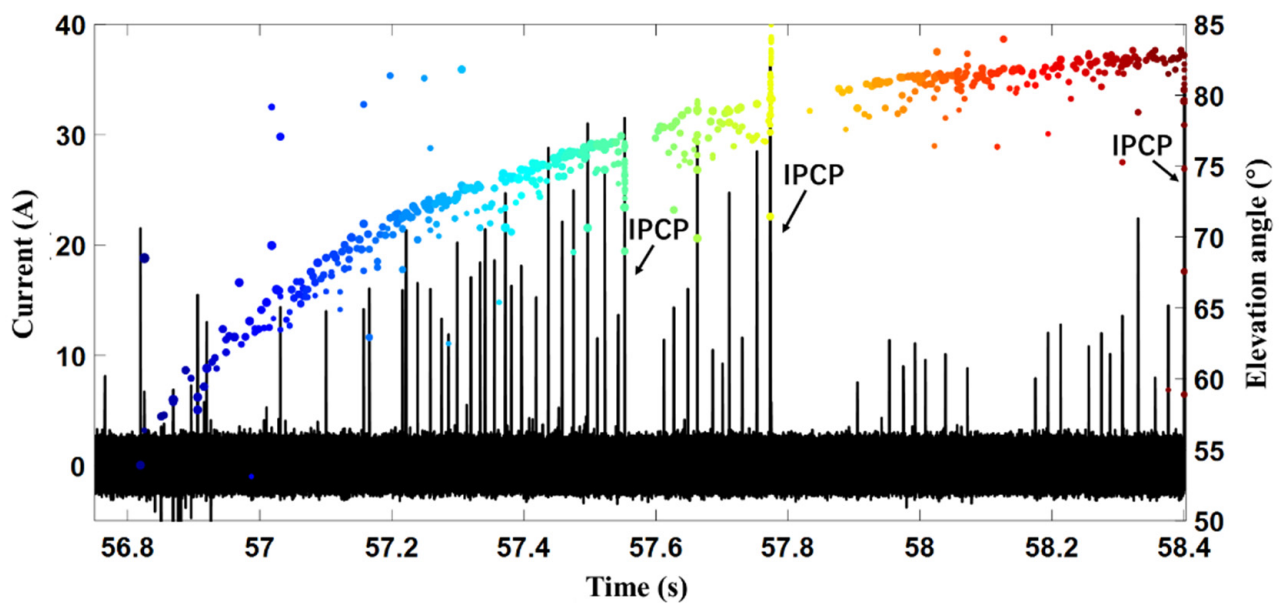of the rocket, and the UPL began self-sustaining development again, but the duration was still very short.

Figure 12. Elevation positioning results and current of the initial stage of triggered lightning No. 570. The size of the positioning point represents the intensity of VHF radiation, and the color represents time.

After the second self-sustaining development, similar to the first one, there was a quiet period with no obvious pulse in the current waveform, which lasted about 129.13 ms. No VHF radiation source was detected during this period. As the rocket continued to rise, the third initial process began, and the breakdown still occurred near the tip of the rocket. When the third IPCP occurred, the height was about 684 m. At this point, the initial stage of this UPL was over.

Next, the development process of a PCP cluster in the initial stage of lightning No. 570 was analyzed. Figure 13 is the current and the elevation angle of radiation source of this PCP cluster. The PCP cluster contained six current pulses, with a total duration of about 112 μs and an average pulse interval of about 18.1 μs. Assuming that the radiation source developed vertically, the velocity between adjacent pulses in this PCP cluster was on the order of 10^6 m/s. This development speed was far greater than the rising speed of rocket and close to the development speed of IPCP. It can be inferred that PCP clusters were not multiple PCPs that occurred continuously. This may be similar to an IPCP, which is a sign of self-sustaining development of UPL. Usually, there are only 2–3 current pulses in a PCP cluster. In a few cases, there are 4–6 current pulses. The average is 3. A PCP cluster is not accompanied by an ICC process. Therefore, the duration of self-sustaining development is extremely short, and no obvious self-sustaining development channel was found in the PCP cluster in this paper.

In this paper, the first and second self-sustaining developments in the initial stage of triggered lightning No. 570 were defined as short-term self-sustaining development. A process with short duration and weak ICC intensity will not cause wire fusing.

Figure 14 shows the current and positioning results of the first short-term self-sustaining development (IPCP–ICC) process. It can be seen that, with the rise of the rocket, the radiation source in the initial stage continued to develop upward. When the IPCP signal appeared, the UPL developed from the top of the rocket to the direction away from the CINTF antenna (the elevation angle gradually decreases). Based on the elevation angle and azimuth angle of the radiation source detected by CINTF, it was calculated that the two-dimensional speed of the short-term self-sustaining development was on the order of 10^5 m/s.
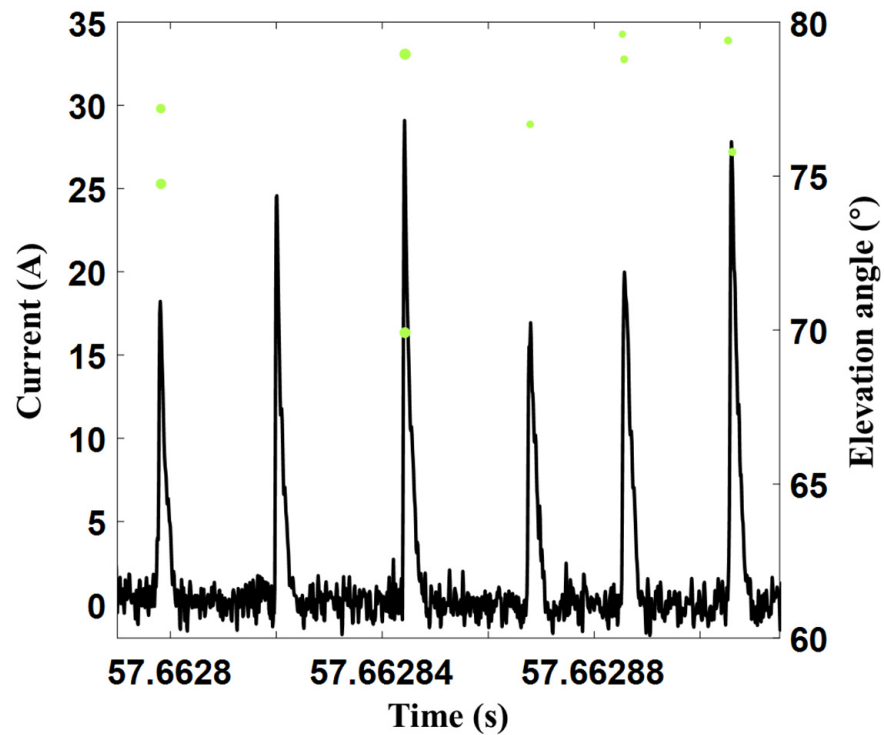
Figure 13. The current and elevation angle of radiation source of a PCP cluster in lightning No. 570. The size of the positioning point represents the intensity of VHF radiation, and the color represents time.
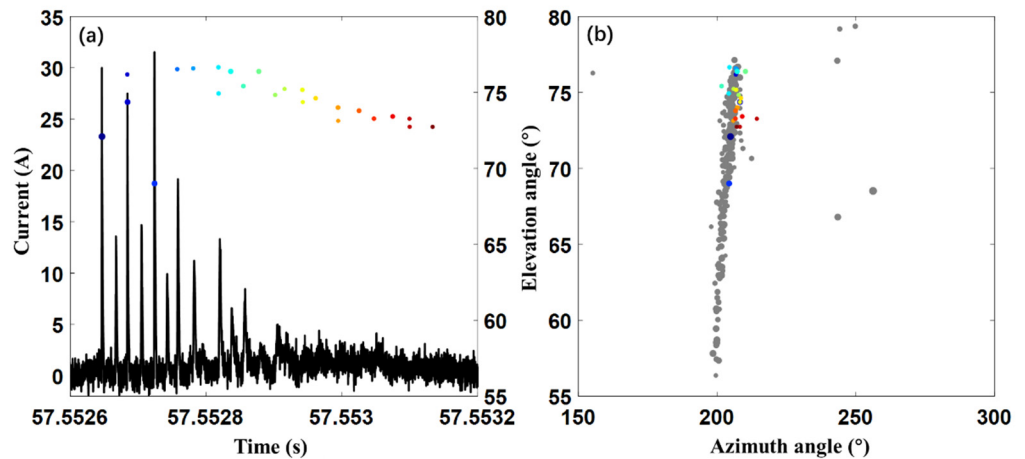

Figure 14. The current waveform and radiation source positioning results of the fist short-term self-sustaining development in lightning No. 570. (**a**) current waveform and elevation of VHF radiation source versus time; (**b**) elevation of VHF radiation sources versus azimuth. The color positioning point is the VHF radiation source of short-term self-sustaining development, and the gray positioning point is the VHF radiation source of the previous initial process. The size of the positioning point repre-sents the intensity of VHF radiation, and the color represents time.

Figure 15 shows the current and positioning results of the second short-term self-sustaining development. It can be seen that both the elevation angle and the azimuth angle of the radiation source increased in this self-sustaining development, which indicates that the UPL was developing westward and upward. The two-dimensional speed of this short-term self-sustaining development was on the order of 10^6 m/s, which is larger than that of the first short-term self-sustaining development. This may be related to the long duration of ICC. During the ICC stage, the development speed of the leader is gradually

accelerated. In addition, at this time, the large elevation angle detected by the CINTF may also lead to a large error.
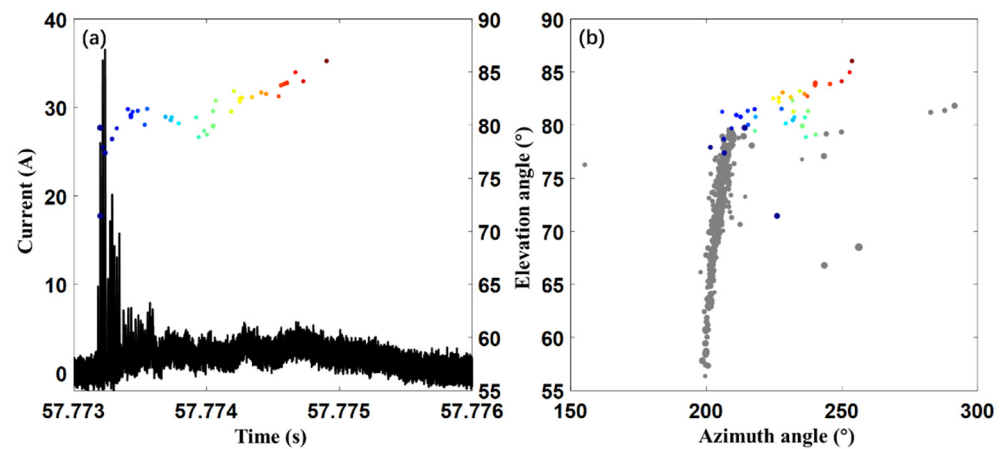

Figure 15. The current waveform and radiation source positioning results of the second short-term self-sustaining development in lightning No. 570. (**a**) current waveform and elevation of VHF ra-diation source versus time; (**b**) elevation of VHF radiation sources versus azimuth. The color posi-tioning point is the VHF radiation source of short-term self-sustaining development, and the gray positioning point is the VHF radiation source of the previous initial process. The size of the posi-tioning point represents the intensity of VHF radiation, and the color represents time.

5. Conclusions

The positioning error of a CINTF for a close-range radiation source was analyzed, and the positioning error calibration method of a CINTF for a specific close-range radiation source was proposed. On the basis of the research results by directly measured current [4], the initial stage of UPL was further observed and studied using a CINTF, and a deeper un-derstanding of the physical process of the initial stage was obtained. The main conclusions are as follows:

1. The calibration method of a CINTF for positioning a specific short-range radiation source was proposed, and the calibration of the CINTF positioning results for the initial stage of the UPL was realized. The positioning error of the short-range radiation source caused by the basic principle of CINTF positioning was analyzed. When the azimuth angle and projection distance of the radiation source were constant, the vertical distance error of CINTF obviously increased with the increase in the elevation angle (height) of the radiation source. When the azimuth and height of the radiation source were constant, the vertical distance error of CINTF decreased obviously with the increase in the projection distance of the radiation source. For long-distance radiation sources, the vertical error of CINTF positioning was within 10 m, which shows the reliability of the conventional results of CINTF positioning. For a short-distance radiation source, the calibration method proposed in this paper improved the observation accuracy. When the elevation angles of the initial stage of the UPL were 40°, 50°, and 60°, the calibrated positioning error in altitude could be reduced by about 11 m, 14 m, and 20 m, respectively.
2. The physical processed during the initial stage of the UPL of triggered lightning with a single initiation process and multiple initiation process were analyzed. When the rocket rose to a certain height, the CINTF began to detect the breakdown discharge process. The PCP signal, generated by a weak upward positive breakdown and a subsequent strong downward negative breakdown near the rising rocket tip, appeared in the current waveform. As the rocket continued to rise, the electric field near the rocket top increased, and PCP clusters appeared in the current waveform. At this time, the UPL began self-sustaining development, but the self-sustaining development disappeared quickly without continuous current. As the rocket continued to rise, the

IPCP signal appeared, indicating that the UPL began self-sustaining development. The self-sustaining development after the IPCP could be short-term or continuous. After the short-term self-sustaining development, breakdown discharge could occur again near the rocket tip. It is also possible that the initial process could end completely and not develop into continuous self-sustaining development.

Although only the errors caused by the assumption of plane wave during CINTF positioning were considered when calibrating the positioning results, existing research have verified the accuracy of the CINTF used in this study [14,16]. Recently, Shao et al. [32] analyzed the uncertainty of general noncoplanar antenna arrays and discussed the effect of antenna layout, radiation source location, and time error on accuracy. In the future, we will further analyze the impact of these factors on the positioning of CINTF. The spatial–temporal resolution of the positioning results can be further improved by changing the antenna layout, increasing the sampling rate of the system, and optimizing the signal processing algorithm. In addition, this research on the initial stage of UPL of triggered lightning is mainly based on fine CINTF positioning. Considering the high spatial resolution of close-range optical observation, it is planned to simultaneously carry out high-speed camera observations in future research.

How lightning initiates is one of the greatest unsolved problems in the atmospheric sciences. Some studies have attempted to observe the initial process of natural lightning. Particularly in recent years, researchers have been able to image the development of lightning flashes with meter-scale accuracy and unprecedented detail with the low-frequency array (LOFAR) [33,34]. These results further shed light on the initial process of natural lightning. In addition, there have been many studies on the initial stage of positive leader based on a long-gap discharge in a high-voltage laboratory. In the future, we can further analyze the similarities and differences of the characteristics and development process of the initial stage with respect to a long-gap discharge in a high-voltage laboratory, natural lightning, and triggered lightning, and further reveal the micro corona streamer mechanism.

Author Contributions: Conceptualization, Y.Z.; methodology, Y.Z. and Z.C.; investigation, Z.C.; data curation, Y.Z., Z.C., Y.F., J.W., W.L., D.Z. and W.P.; writing—original draft preparation, Z.C.; writing—review and editing, Y.Z.; funding acquisition, Y.Z. All authors have read and agreed to the published version of the manuscript.

Informed Consent Statement: Not applicable.

Data Availability Statement: The data can be obtained from the corresponding author (zhangyang@cma.gov.cn).

Conflicts of Interest: The authors declare no conflict of interest.

References

1. Horii, K. Experiment of artificial lightning triggered with rocket. *Mem. Fac. Eng. Nagoya Univ.* **1982**, *34*, 77–112.
2. Willett, J.C.; Davis, D.A.; Laroche, P. An experimental study of positive leaders initiating rocket-triggered lightning. *Atmos. Res.* **1999**, *51*, 189–219. [CrossRef]
3. Zhang, Y.; Qian, Y.; Zhang, Y.; Lyu, W.; Zheng, D.; Chen, S. Discharge characteristics of upward positive leaders in initial stage of artificially triggered lightning. *High Volt. Eng.* **2017**, *43*, 1602–1608. (In Chinese)
4. Chen, Z.; Zhang, Y.; Fan, Y.; Wang, J.; Zheng, D.; Fan, X.; Xu, L.; Lyu, W.; Zhang, Y. Evolution characteristics during initial stage of triggered lightning based on directly measured current. *Atmosphere* **2020**, *11*, 658. [CrossRef]

5. Li, X.; Lu, G.; Jiang, R.; Zhang, H.; Fan, Y.; Shi, T.; Qie, X.; Zhang, Y.; Ren, H.; Zhang, C.; et al. On the transition from precursors to the initial upward positive leader in negative rocket-triggered lightning. *J. Geophys. Res. Atmos.* **2021**, *126*, e2020JD033926. [CrossRef]

6. Shao, X.M.; Rhodes, C.T.; Holden, D.N. Rf radiation observations of positive cloud-to-ground flashes. *J. Geophys. Res.* **1999**, *104*, 9601–9608. [CrossRef]

7. Ushio, T.-O.; Kawasaki, Z.-I.; Ohta, Y.; Matsuura, K. Broad band interferometric measurement of rocket triggered lightning in Japan. *Geophys. Res. Lett.* **1997**, *24*, 2769–2772. [CrossRef]

8. Dong, W.; Liu, X.; Zhang, Y. Broadband interferometer observation of an artificially triggered lightning. *Chin. Sci. Bull.* **2001**, *46*, 427–432. (In Chinese) [CrossRef]

9. Yoshida, S.; Biagi, C.J.; Rakov, V.A.; Hill, J.D.; Stapleton, M.V.; Jordan, D.M.; Uman, M.A.; Morimoto, T.; Ushio, T.; Kawasaki, Z.-I. Three-dimensional imaging of upward positive leaders in triggered lightning using VHF broadband digital interferometers. *Geophys. Res. Lett.* **2010**, *37*, L05805. [CrossRef]

10. Edens, H.E.; Eack, K.B.; Eastvedt, E.M.; Trueblood, J.J.; Winn, W.P.; Krehbiel, P.R.; Aulich, G.D.; Hunyady, S.J.; Murray, W.C.; Rison, W.; et al. VHF lightning mapping observations of a triggered lightning flash. *Geophys. Res. Lett.* **2012**, *39*, L19807. [CrossRef]

11. Hill, J.D.; Pilkey, J.; Uman, M.A.; Jordan, D.M.; Rison, W.; Krehbiel, P.R. Geometrical and electrical characteristics of the initial stage in Florida triggered lightning. *Geophys. Res. Lett.* **2012**, *39*, L09807. [CrossRef]

12. Hill, J.D.; Pilkey, J.; Uman, M.A.; Jordan, D.M.; Rison, W.; Krebhiel, P.R.; Biggerstaff, M.I.; Hyland, P.; Blakeslee, R. Correlated lightning mapping array and radar observations of the initial stages of three sequentially triggered Florida lightning discharges. *J. Geophys. Res. Atmos.* **2013**, *118*, 8460–8481. [CrossRef]

13. Sun, Z.; Qie, X.; Jiang, R.; Liu, M.; Wu, X.; Wang, Z.; Lu, G.; Zhang, H. Characteristics of a rocket-triggered lightning flash with large stroke number and the associated leader propagation. *J. Geophys. Res. Atmos.* **2014**, *119*, 13388–13399. [CrossRef]

14. Zhang, Y.; Krehbiel, P.R.; Zhang, Y.; Lu, W.; Zheng, D.; Xu, L.; Huang, Z. Observations of the initial stage of a rocket-and-wire-triggered lightning discharge. *Geophys. Res. Lett.* **2017**, *44*, 4332–4340. [CrossRef]

15. Zhang, Y.; Yang, S.; Lu, W.; Zheng, D.; Dong, W.; Li, B.; Chen, S.; Zhang, Y.; Chen, L. Experiments of artificially triggered lightning and its application in Conghua, Guangdong, China. *Atmos. Res.* **2014**, *135–136*, 330–343. [CrossRef]

16. Zhang, Y.; Zhang, Y.J.; Zheng, D.; Lu, W. Characteristics and discharge processes of m events with large current in triggered lightning. *Radio Sci.* **2018**, *53*, 974–985. [CrossRef]

17. Zhang, Y.; Zhang, Y.; Xie, M.; Zheng, D.; Lu, W.; Chen, S.; Yan, X. Characteristics and correlation of return stroke, M component and continuing current for triggered lightning. *Electr. Power Syst. Res.* **2016**, *139*, 10–15. [CrossRef]

18. Zhang, Y.; Zhang, Y.; Li, C.; Lu, W.; Zheng, D. Simultaneous optical and electrical observations of "chaotic" leaders preceding subsequent return strokes. *Atmos. Res.* **2016**, *170*, 131–139. [CrossRef]

19. Zhang, Y.; Zhang, Y.; Zheng, D.; Lu, W. Preliminary breakdown, following lightning discharge processes and lower positive charge region. *Atmos. Res.* **2015**, *161–162*, 52–56. [CrossRef]

20. Zheng, D.; Zhang, Y.; Zhang, Y.; Lu, W.; Yan, X.; Chen, S.; Xu, L.; Huang, Z.; You, J.; Zhang, R.; et al. Characteristics of the initial stage and return stroke currents of rocket-triggered lightning flashes in southern China. *J. Geophys. Res. Atmos.* **2017**, *122*, 6431–6452. [CrossRef]

21. Rison, W.; Krehbiel, P.R.; Stock, M.G.; Edens, H.E.; Shao, X.M.; Thomas, R.J.; Stanley, M.A.; Zhang, Y. Observations of narrow bipolar events reveal how lightning is initiated in thunderstorms. *Nat. Commun.* **2016**, *7*, 10721. [CrossRef] [PubMed]

22. Shao, X.M.; Holden, D.N.; Rhodes, C.T. Broad band radio interferometry for lightning observations. *Geophys. Res. Lett.* **1996**, *23*, 1917–1920. [CrossRef]

23. Rhodes, C.T.; Shao, X.M.; Krehbiel, P.R.; Thomas, R.J.; Hayenga, C.O. Observations of lightning phenomena using radio interferometry. *J. Geophys. Res.* **1994**, *99*, 13059–13082. [CrossRef]

24. Shao, X.M.; Krehbiel, P.R.; Thomas, R.J.; Rison, W. Radio interferometer observations of cloud-to-ground lightning phenomena in Florida. *J. Geophys. Res.* **1995**, *100*, 2749–2783. [CrossRef]

25. Biagi, C.J.; Jordan, D.M.; Uman, M.A.; Hill, J.D.; Beasley, W.H.; Howard, J. High-speed video observations of rocket-and-wire initiated lightning. *Geophys. Res. Lett.* **2009**, *36*, L15801. [CrossRef]

26. Biagi, C.J.; Uman, M.A.; Hill, J.D.; Jordan, D.M. Observations of the initial, upward-propagating, positive leader steps in a rocket-and-wire triggered lightning discharge. *Geophys. Res. Lett.* **2011**, *38*, L24809. [CrossRef]

27. Biagi, C.J.; Uman, M.A.; Hill, J.D.; Rakov, V.A.; Jordan, D.M. Transient current pulses in rocket-extended wires used to trigger lightning. *J. Geophys. Res.* **2012**, *117*, D07205. [CrossRef]

28. Lalande, P.; Bondiou-Clergerie, A.; Laroche, P.; Eybert-Berard, A.; Berlandis, J.-P.; Bador, B.; Bonamy, A.; Uman, M.A.; Rakov, V.A. Leader properties determined with triggered lightning techniques. *J. Geophys. Res.* **1998**, *103*, 14109–14115. [CrossRef]

29. Zhang, Y.; Chen, Z.; Wang, J.; Fan, Y.; Zheng, D.; Lyu, W.; Zhang, Y. Observation of the whole discharge process during a multi-stroke triggered lightning by continuous interferometer. *J. Appl. Meteorol. Sci.* **2020**, *31*, 197–212. (In Chinese)

30. Abarca, S.F.; Corbosiero, K.L.; Galarneau, T.J., Jr. An evaluation of the Worldwide Lightning Location Network (WWLLN) using the National Lightning Detection Network (NLDN) as ground truth. *J. Geophys. Res.* **2010**, *115*, D18206. [CrossRef]

31. Jiang, R.; Qie, X.; Wang, C.; Yang, J. Propagating features of upward positive leaders in the initial stage of rocket-triggered lightning. *Atmos. Res.* **2013**, *129–130*, 90–96. [CrossRef]

32. Shao, X.-M.; Ho, C.; Meierbachtol, C.S.; Anderson, D. Lightning interferometric processing and uncertainty analysis for general noncoplanar antenna arrays. *Earth Space Sci. Open Arch.* **2021**, 16.

33. Scholten, O.; Hare, B.M.; Dwyer, J.; Sterpka, C.; Kolmašová, I.; Santolík, O.; Lán, R.; Uhlíř, L.; Buitink, S.; Corstanje, A.; et al. The initial stage of cloud lightning imaged in high-resolution. *J. Geophys. Res. Atmos.* **2021**, *126*, e2020JD033126. [CrossRef]

34. Sterpka, C.; Dwyer, J.; Liu, N.; Hare, B.M.; Scholten, O.; Buitink, S.; Veen, S.T.; Nelles, A. The spontaneous nature of lightning initiation revealed. *Geophys. Res. Lett.* **2021**, *48*, e2021GL095511. [CrossRef]